Influence of Al_2O_3 addition on thermal and structural properties of erbium doped glasses

A. BONAMARTINI CORRADI, V. CANNILLO, M. MONTORSI, C. SILIGARDI*
Dipartimento di Ingegneria dei Materiali e dell'Ambiente, Università di Modena e Reggio Emilia, via Vignolese 905, 41100, Modena, Italy
E-mail: siligardi.cristina@unimore.it

Published online: 21 April 2006

Changes in the structural properties of Er^{3+} doped soda-lime silicate glasses were investigated as a function of Al_2O_3 content. A combined approach of experimental techniques and molecular dynamic simulations (MD) was used to evaluate the structural features directly correlated to the glass properties. The experimental results in term of density, thermal properties as well as microstructural and mineralogical data showed a significant variation when increasing the alumina content from 10 mol% to 15 mol%. These results were compared to the MD information and discussed: changes in erbium and aluminium local configuration, due to the glass structural evolution as a function of the alumina concentration, have been investigated.

1. Introduction

Rare earth containing glasses have attracted a great deal of interest due to their important physical and chemical properties. Such glasses are heat and mechanically resistant, chemically stable and show interesting optical and magnetic properties. Recently, this class of glasses has been widely studied for optical communications [1], laser technology [2], and immobilization of radioactive [3] materials. In particular Er-doped glass fibres as laser and, more importantly, as optical amplifiers in all-optical long-distance telecommunication fibres networks, have received considerable attention.

Silicate glasses have still to be considered an excellent host for lanthanide ions, especially for the development of integrated optical amplifiers and lasers, due to their chemical robustness and adaptability to different waveguide fabrication processes.

In this work, several compositions belonging to the soda-lime erbium doped system have been considered: increasing percentages of alumina (5–20% mol) have been added to the base composition. The ratio between Na_2O to CaO has been kept constant for all the compositions. The relative large content of alkali is justified since the purpose is to produce waveguides by using the ion-exchange process. The optical and spectroscopic properties of these glasses have been thoroughly studied [4–7], and, in particular, the use of the soda-lime glass for optical amplifiers has been investigated [5]. Low propagation losses (lower than 0.2 dB/cm at 1.5 μm wavelength) have been achieved, and preliminary measurements have shown that optical gain of a fraction of dB/cm is attainable using only a few tens of mW of pump power at 1 μm [7]. These results indicated that these materials have good perspectives of technological application; therefore the understanding and control over structurally related properties become extremely important. In this work, the definition of the structural features directly responsible of the material behaviour relies on a combined approach of experimental and simulation techniques. Computer simulation is essential in the case of complex materials with absence of long range order. In particular, molecular dynamic simulations, allowing the study at the atomistic level, can be used to characterize the short range environment of the glass network. It is well known that the RE ions tends to clusterize into the glass network, favouring the energy transfer between neighbouring ions. This phenomenon leads to the concentration quenching of luminescence experimentally observed [2]. It was previously discussed that the addition of alumina in the glass composition improves the optical response of the material as a results of structural changes involving the rare earth based clusters [8].

The addition of an extra cation to the glass network exerts an influence on the glass structure because it directly influences the cross-linking between polyhedra constituting the three dimensional network. In particular the ratio between oxygen linked to one or two

*Author to whom all correspondence should be addressed.
0022-2461
DOI: 10.1007/s10853-006-6119-5

network former cation, defined respectively as non bridging oxygen (NBO) and bridging oxygen (BO), changes as a function of the species introduced in the glass matrix. The aluminium acting as a network former promotes the NBO conversion into BO species: the different electron-donating abilities of oxygen ions between Si–NBO and Si–O–Si or Si–O–Al species is the main reason of the change in optical parameters [9].

In this work the structural evolution induced by the alumina addition has been studied and the modifications occurring in the aluminium and the erbium site have been analysed in order to understand the structural related optical properties [10].

Changes in thermal and physical properties as a function of alumina addition to the base composition have been measured and the experimental data have been compared to the MD structural information.

2. Experimental procedure

2.1. Glasses preparation

The examined compositions are given in Table I.

The batches were prepared by using reagent grade SiO_2, Na_2CO_3, K_2CO_3, Al_2O_3, $CaCO_3$, $(NH_4)_3PO_4$, and Er_2O_3 as starting materials. Batches, previously dry milled, were melted in an electrically heated furnace (Lenton, mod. EHF 17/17) within Pt crucibles, following the same heating cycle: From 20 to 1000°C at 10°C/min, with a 24 h soaking time at 1000°C, from 1000 to 1550°C at 20°C/min and finally 1 h of soaking time at the maximum temperature of 1550°C. The melted batches were quenched in a graphite mould to obtain small pieces of glass having a bar form, and in water in order to obtain frits. To prepare the glass-ceramics, all samples were inserted into the muffle kiln (Remet mod. Melt-two) at room temperature, and consecutively heated at 10°C/min up to 1000°C, with 30 min soaking time. Specimens were then placed on refractory brick up to room temperature.

2.2. Glass characterisation

The densities of the glass specimens were measured by Helium Picnometer (Micromeritics, Mod. AccuPyc 1330) on five different samples for each glass composition. In processing the experimental data the unit molar volume (V_1), was calculated to acquire information about the structural compactness. In a multicomponent glass, as it is the case, the unit volume V_1 is expressed as:

$$V_1 = V_M/n_O = W_g/(\rho \times n_O)$$

where V_M is the molar volume of glass (cm^3/mol), n_O is the mean number of oxygen ions (Σ molar fraction $\times$ number of oxygen per each oxide), W_g is the molar weight of glass (Σ molar fraction $\times$ molecular weight of each single oxide) and ρ is the experimental density obtained by Helium picnometry [11]. The reciprocal value of V_1 signifies the number of oxygen gram atoms per cm^3 of glass (O cm^{-3}) which also depends simultaneously on the density of cross-linking, *DN*. With a multicomponent silicate glass containing alumina, this value is calculated by the formula:

$$DN = 6 - [2/(N_{Si} + N_{Al})]$$

where $N_M = m_{M,i}\ m_i/\Sigma\ n_{O,i}\ m_i$, ($M$ = Si; Al) being m_i the molar percent, $m_{M,i}$ number of atoms of the electropositive element in the i^{th} oxide molecule M_mO_n, $n_{O,i}$ number of oxygen atoms in the same i^{th} oxide. So, from the adopted expression, the density of cross-linking, DN, is expressed by the number of excessive bridging oxygen per the central ion of the network-forming element, Si and Al for alumino-silicates [11].

The glass transition and crystallisation temperatures were determined with a Netzsch, STA 409 differential thermal analyser (DTA) on samples ground to an average particle size of less than 25 μm. The DTA measurements were carried out on about 30 mg of sample in a Pt crucible. Data for each run were automatically collected from the DTA apparatus.

To detect the crystalline phases formed during the heat treatment, X-ray diffraction (XRD) was performed on finely ground glass-ceramic specimens. Patterns were collected using a powder diffractometer (Philips PW3710) with a Ni-filtered Cu Kα radiation in the 10–50° 2Θ range, step size 0.02°, 3 s time step. Information concerning the mechanism of crystallisation and the microstructure of the glass-ceramic materials were obtained by a scanning electron microscopy, SEM, (Philips, XL 40) on cross-section polished and surface gold-coated specimens.

TABLE I Compositions of studied materials in mol%

	1Al*	5Al	10Al	15Al	20Al
SiO_2	72.64	69.84	66.64	63.71	61.14
Na_2O	13.94	13.40	12.79	12.23	11.73
CaO	10.96	10.54	10.05	9.61	9.23
Al_2O_3	0.99	4.81	9.17	13.16	16.67
P_2O_5	0.40	0.38	0.37	0.35	0.33
K_2O	0.60	0.58	0.55	0.53	0.51
Er_2O_3	0.47	0.45	0.43	0.41	0.39

*base glass.

2.3. Computational procedure

The molecular dynamics technique is based on the solution of the Newton's equation of motion for an ensemble of particles constituting the input structure. In the simulation box the atoms are treated according to the Born model of solids [12] where the interactions between pairs of atoms have been codified by parameterized potential functions based on Vessal's model [13]. While the covalent nature of the inter atomic bonding has been considered by using a three body Screened Vessal potential, for the short

range interaction a parameterized Buckingham potential has been employed [13, 14]. In this work, to simplify the MD calculation, input structures have been obtained adding the contribution of the K_2O (mol%) to the mol% of Na_2O and the mol% of P_2O_5 to the SiO_2 (mol%).

The starting structure has been melted at 12000 K in order to remove the memory of the initial configuration [15] and the simulation at this temperature runs in two times: The first in which the O–Si–O three body terms has been omitted and the second time in which the O–Si–O term has been introduced to take into account the covalent nature of the bond [16]. To obtain the final glass structure the system has been cooled, going through several intermediate temperatures corresponding to 9000, 7000, 5000, 3000 and 1500 K, to reach the room temperature (298 K). The annealing schedule consists of 20000 time steps relaxations at each temperature: During the first 6000 time steps the velocity is scaled every time step, during the second 6000 time steps the velocity is scaled every 40 time steps and during the last 8000 time steps no velocity scaling is performed. The room temperature simulation has been done for 30000 time steps and the data collection has been performed during the last 10000 time steps.

A time step of 2×10^{-15} s has been used for a total number of 170000 time steps corresponding to 340 ps with a nominal cooling rate of 3.52×10^{13} K/s [16–17]. The canonical ensamble (NVT), employing the Evans thermostat, has been used at high temperature and the microcanonical ensamble (NVE) has been considered from 3000 K to 298 K [15–18].

The local environment of the glass materials has been investigated in terms of pair distribution function (PDF) and averaged coordination number (CN) of the different species in the glass with particular attention to the aluminium and silicon ions. The short range order (SRO) configuration has been further analysed considering the bond angle distribution (BAD). This parameter allows to quantify the distortion of the polyhedra constituting the glass network as a function of the alumina addition [15]. The SRO characterization has been completed by the BO (bridging oxygens) NBO (non-bridging oxygens) and TBO (three bridging oxygens) distribution analysis. These species are defined on the network former ion-oxygen bond distance criteria: the non bridging oxygens (NBO) are species linked to only one network former ion, the bridging oxygens (BO) are oxygens linked to two network former ions and finally the three bridging oxygens (TBO) are oxygens linked to three network former ions [15–16].

3. Results and discussion

The effects of the alumina addition to the glass sample have been investigated by using different techniques.

Density measurements are sensitive to the glass composition variation more than to other physical properties of glasses. In general, the addition of extra ions in the glass structure results in the modification of the density of the final material. In particular, this effect is strongly related to the mass of the added ions as a function of their content in the base glass [19]. The variation of the glass density induced by the alumina addition, reported in Table II, shows a general increase of the experimental density as a function of the alumina concentration in the glass. It is possible to note that going from 1Al to10Al the density remains almost constant, whilst for the 15Al and 20Al samples a significant increase of the values can be observed.

TABLE II Density and DN of studied samples

Sample	Density (g/cm^3)	D_N
1Al	2.5532 ± 0.0003	2.09
5Al	2.5584 ± 0.0003	2.12
10Al	2.5520 ± 0.0004	2.22
15Al	2.6230 ± 0.0001	2.29
20Al	2.6233 ± 0.0001	2.35

The density depends not only on the packaging space with mass, but also on the atomic weight; therefore a comparison between glasses that contain oxides with similar molar weights can be done (eg SiO_2, CaO, Na_2O). Glasses containing different molar weights components (e.g containing K_2O, MgO, Al_2O_3) can be compared in terms of molar volume V1 related to 1 gram atom of oxygen [20] and expressed in cm^3 per gram atom of O^{2-}. Moreover the volume packaging of glass particles can be extrapolated by the glass volume analysis. The glass has been considered as a polymer in which the oxygens are bound into a network of electropositive elements exhibiting a prevalence of covalent bonds:

a) with various degrees of cross-linking of components
b) with various densities of spatial cross-linking
c) with varying free space between the particles
d) with various cross-linkage strength.

Plotting the values of V1 versus the concentration of the oxide, in mol%, it is possible to obtain 3 curves in 3 possible extreme positions.

If the curve is more or less parallel to the x axis, all the atoms of electropositive elements are situated in the cavities of the silica network or an isomorphous substitution for SiO_2 is involved (e.g. with Al_2O_3).

When the curve is ascending, the silica network is expanded by the entry of other elements: in other words the unit volume V1 is increased by the entry of the elements. A descending curve means that the mass of elements leads to a shrinkage of the silica network which has been shown in particular for elements with a small effective radius r_i. Fig. 1 reports V1 as a function of the Al_2O_3 concentration for the studied glasses. It is possible to note that while up to 10 mol% the V1 values are quite similar, at higher concentration the V1 values decrease. The addition of low percentage of alumina seems not to change significantly the glass structure but in the 15Al and 20Al samples a

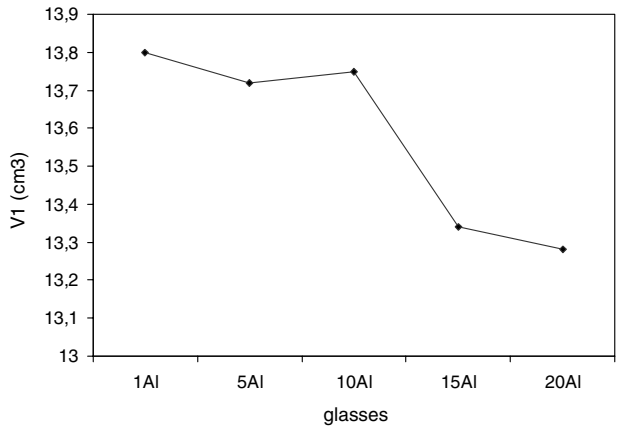

Figure 1 V1 of the investigated glasses.

strong influence in the packaging of the atoms can be observed as a function the aluminium addition. This ion, acting as a network former, promotes the molar volume decrease.

The molecular dynamics results, expressed in terms of the averaged coordination number of aluminium, indicates a fourfold coordination for this ion confirming its network former role in the glass materials. Table III reports the three, four and five contributions to the averaged coordination number of the Al^{3+} and it is possible to observe that while for the 1Al, 5Al and 10Al samples the contribution of the five folded aluminium remains practically constant, in the glasses with the higher alumina content the percentage of the five coordinated aluminium increases. This result can be explained considering that the alumina addition promotes a structural evolution characterized by the creation of new cross linking between the Al^{3+} based tetrahedra, constituting the three dimensional network, with a consequent increase of the degree of polymerization of the material. This result, in agreement with the experimental density, allows to confirm that in these materials the aluminium ions play a network former role increasing the glass compactness especially for Al_2O_3 content >10 mol%.

Molecular dynamics results also indicate an averaged coordination number of 4 for the silicon atoms and in this case the contribution to the coordination number is independent from the alumina concentration in the glass matrix (data not reported). While the silicon site seems not to be affected by the alumina addition in the glass matrix, the aluminium one shows significant changes at higher alumina concentrations going toward a more interconnected configuration.

The increasing polymerization of the glass network is also pointed out by the analysis of the BO, NBO and TBO contribution to the aluminium and silicon coordination number reported in Table IV.

The main contribution to the aluminium coordination is ascribed to BO species but while for the 1Al and 5Al samples the TBO contribution is negligible, for the 10Al, 15Al and 20Al samples the TBO contribution rapidly increases. In particular, for higher alumina contents the TBO increase partially balances the BO species decrease. As previously discussed [21], the presence of TBO species in the first coordination shell of an ion is associated to the increased polymerization of the glass network in agreement with the network former role played by the aluminium in these systems. As regard the Si coordination number, the main contribution is due to the BO species and the NBO decrease, observed as a function of the alumina addition, but is partially compensated by the Si-TBO formation. It is worth noting that the main contribution to the TBO species is ascribed to the aluminium ion confirming its network former action in the glass structure as previously pointed out by the V1 analysis.

The increasing polymerization of the glass material is confirmed by the BAD analysis that shows the decrease of the interconnection angle between the Al based tetrahedra as a function of the alumina concentration in the glass composition. In particular the Al–O–Al BAD, reported in Fig. 2, shows the shift of the main peak from 180° to 120° in agreement with the increased compactness of the polyhedra constituting the three dimensional network [22]. The 1Al curve shows an anomalous trend because the small number of Al atoms, according to the low alumina concentration, leads to a non representative behaviour.

The NBO, BO and TBO distribution has been also considered to acquire information on the local environment of the Er^{3+} ion. This ion acts as a network modifier in the glass structure as confirmed by the main contribution to the erbium coordination number ascribed to the NBO species. Moreover Fig. 3 shows a progressive conversion of NBO into BO species, as a function of the alumina concentration, and these changes in the local symmetry around the RE cation are correlated to the optical response of the material.

TABLE III Contribution (percentage) to the aluminium and silicon coordination number

	Al			Si	
Sample	3.00	4.00	5.00	Average	Average
1Al	0.32	98.91	0.77	4.00	4.08
5Al	2.24	97.24	0.52	3.98	4.06
10Al	3.12	96.79	0.09	3.97	4.05
15Al	2.35	94.83	2.82	4.00	4.03
20Al	1.27	89.53	9.08	4.08	4.05

TABLE IV NBO, BO and TBO contribution to the silicon and aluminium coordination number

Sample	Si-NBO	Si-BO	Si-TBO	AlNBO	Al-BO	AlTBO
1Al	17.47	82.51	0.01	0.76	98.81	0.43
5Al	12.96	86.87	0.18	3.74	94.65	1.62
10Al	10.13	89.43	0.43	2.88	93.41	3.71
15Al	7.35	91.55	1.10	1.60	91.89	6.50
20Al	7.35	88.23	4.42	1.18	81.35	17.47

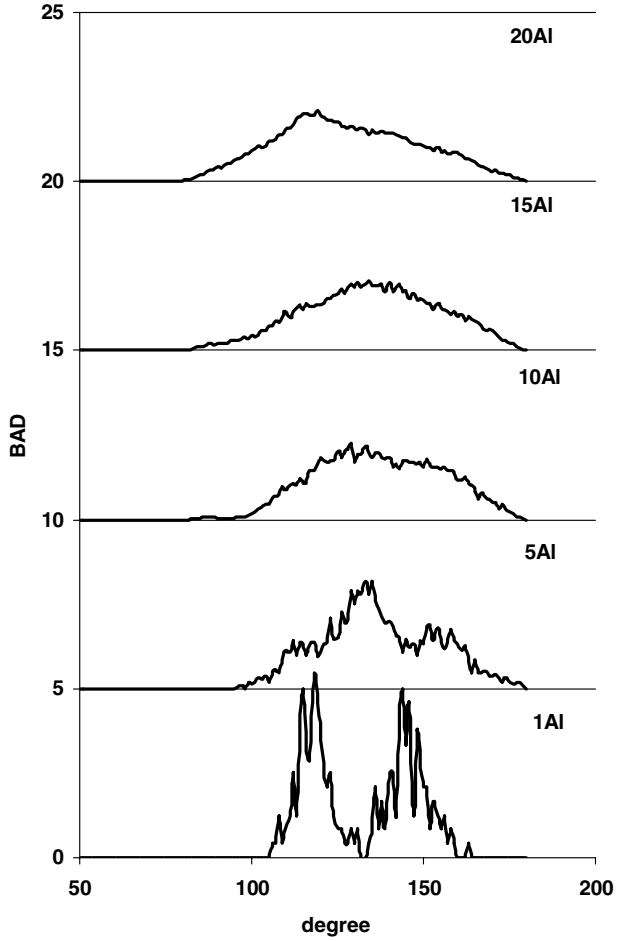

Figure 2 Al-O-Al bond angle distribution.

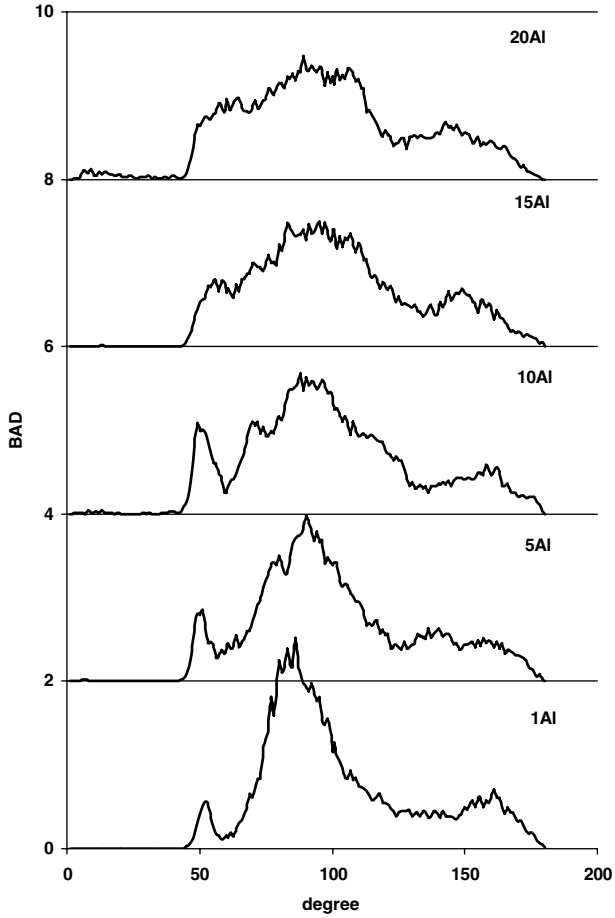

Figure 4 O-Er-O bond angle distribution.

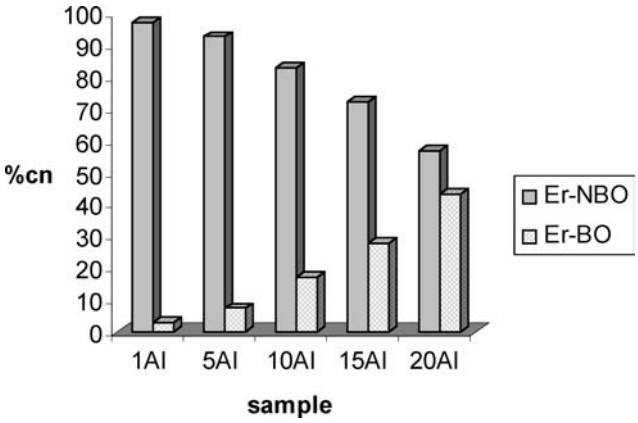

Figure 3 NBO and BO contribution (in percentage) to the erbium coordination number.

The loss of symmetry around the erbium cations has been also confirmed by the O–Er–O BAD reported in Fig. 4. The 1Al sample shows two different maxima, at about 60° and 90° respectively, which correspond to the different angles that this triplet can form in irregular structure. The peak at about 60° increases at the expense of the one at about 90°, as a function of the alumina addition, up to 10% mol of Al. This behaviour can be explained considering that the network former action of the Al^{3+} results in the general increase of the glass polymerization leading to the Er^{3+} based octahedra distortion. For higher alumina content (samples 15Al and 20Al), a broadening of the main peaks can be observed. This result suggests that a concentration of alumina higher than 10% mol promotes a structural evolution in which a random distribution of the Er^{3+} cations takes place. This result is also confirmed by the Er-Er PDF analysis. Previous works demonstrated that the presence of a main peak at about 4 Å is associated to a heterogeneous region in which the rare earth (RE) ions clusterize [12, 16]. In Fig. 5 the PDF curves for three selected samples are reported and it is possible to note that going from 10Al to 20Al the main peak shifts to higher distances. This result can be explained considering that the Al_2O_3 addition promotes the separation of the Er-Er species with homogenization of the RE cations in the glass network. It is worth noting that alumina plays a fundamental role in these glasses and its addition could be used to avoid the phase separation responsible of the quenching of luminescence experimentally observed [9]. Further details about the role of alumina into high Er^{3+} containing glasses are under investigation in order to quantify the alumina concentration to which corresponds specific optical properties useful for technological application [23].

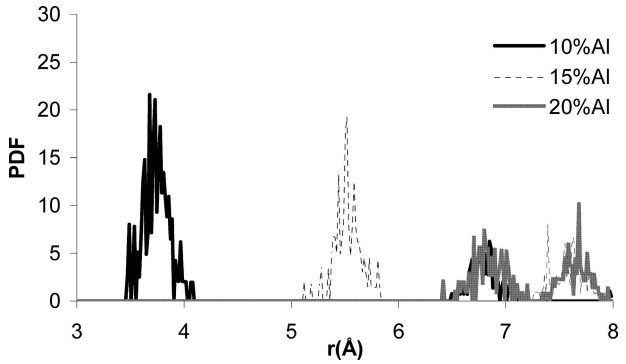

Figure 5 Er-Er pair distribution function for three selected samples.

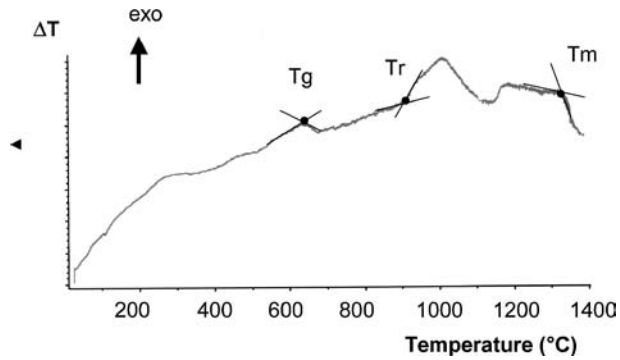

Figure 6 DTA of 10Al sample at the rate of heating 10°C/min: T_g, T_r and T_m are indicated.

DTA thermograms of the studied compositions collected on the powders at a heating rate of 10°C/min present very similar features for the 1Al, 5Al and 10Al samples and for the 15Al and 20Al samples (Table V): (a) an endothermic peak, T_g, corresponding to the glass transformation temperature; (b) exothermic events indicating the crystallisation peak temperatures, T_p.

It is possible to consider that the crystallisation peaks of the samples with low alumina content are broader than those recorded for samples containing 15 and 20 mol% of Al_2O_3. In particular the former present higher T_p peaks. Glass transition temperature T_g and crystallization temperature T_p are remarkably influenced by glass compositions since both temperatures decrease with increasing of alumina content. Rao pointed out that some properties are affected by the degree of cross-linking of the glass network as well as by the type of bonds and by the bonding strength [24]. These properties namely T_g, η, E and α, depend simultaneously on the density of cross-linking DN and the number of oxygens per volume (O cm^{-3}) [11]. Table II reports DN values as a function of the alumina content in the glass samples and the data reported are in agreement with the results obtained from DTA analysis.

An explanation, at least qualitatively, of the results obtained can be proposed in terms of degree of mobility, acquired by the network, to the extent allowed during the transformation interval. The transformation temperature does not change with the glasses having the same density of cross-linking DN. The T_g decreases with decreasing DN while T_g increases with increasing DN. In order to measure the thermal stability of glass, Hruby [25] proposed a method to evaluate the glass-forming tendency on the basis of relative transformation, early crystallization and melting temperature position. These temperatures are determined by means of DTA. One assumes that the glass-forming tendency is expressed numerically by the K_{gl} value calculated by the equation: $K_{gl} = T_r - T_g/T_m - T_r$ where the meaning of the temperatures is reported in Fig. 6. The results obtained from the measurements performed on the glass sample are summarized in Table VI. Values of about 0.1 indicates that the glass formation is very difficult and requires the exact control of the most suitable experimental conditions; if $K_{gl} = 0.5$ the glass is easily prepared by free cooling of the melt in air, while values of $K_{gl} = 1$ and more are related to a high-molecular polymer type glass. A short interval $T_r - T_g$ signifies that the glass contains structural units with high crystallization tendency while a short temperature interval $T_m - T_r$ is indirectly proportional to the glass-forming tendency. In order to confirm the reported results a summary of X-ray patterns for 5Al, 10Al, 15Al and 20Al glasses treated at 1000°C for 30 min is given in Fig. 7. The data reported underlined two different effect of Al_2O_3 on the base glass: while the 5Al and 10Al samples are amorphous, the 15Al and 20Al show an incipient crystallization. It is possible to note that high amount of alumina acts as "nucleant" since the glasses present a very high tendency to devitrify and in particular the crystalline phase is a sodium-aluminosilicate ($NaAlSiO_4$) named nepheline (JCPDS-ICCD 35-0424).

Molecular dynamic simulations can be used to explain the structural modification promoted by the alumina addition in the glass matrix in terms of local configuration of the cations [15, 16, 18]. In particular the attention is

TABLE V DTA results: Temperature in °C

	T_g	T_p
1Al	560	950*
5Al	581	950*
10Al	644	950
15Al	673	927
20Al	700	900

*Weak.

TABLE VI Hruby temperature intervals of the studied samples

Sample	$T_p - T_g$	$T_m - T_p$	K_{gl}
1Al	340	425	0.80
5Al	319	450	0.71
10Al	266	449	0.59
15Al	191	463	0.41
20Al	164	463	0.35

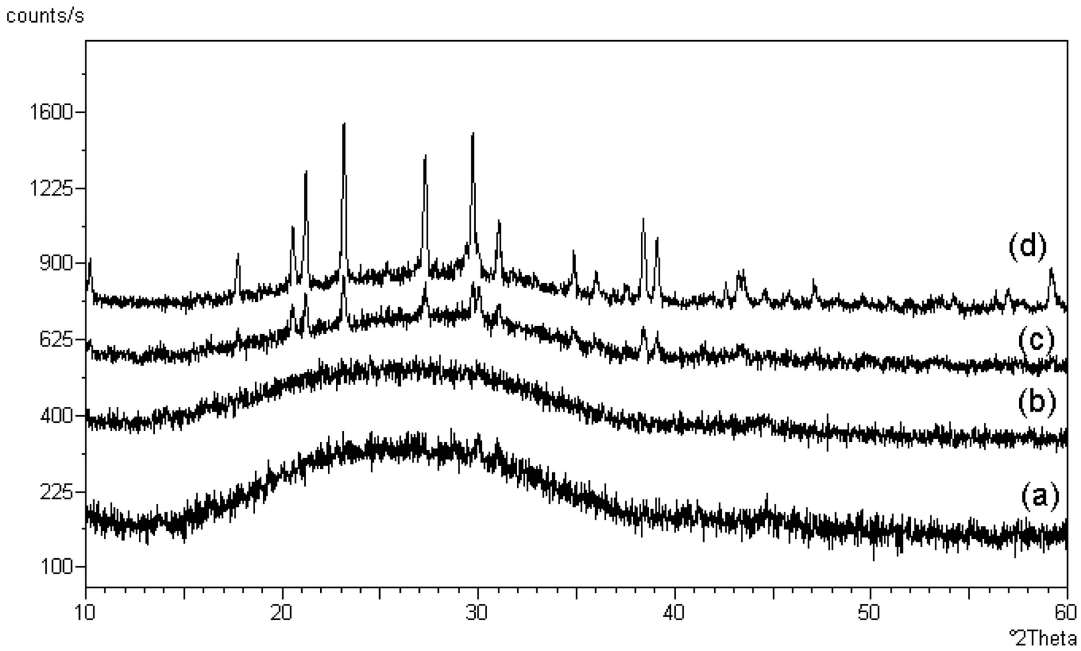

Figure 7 XRD patterns of the samples heat treated at 1000°C for 30 min: (a) 5Al; (b) 10Al; (c) 15Al; (d) 20Al.

directed to study the possibility of the structure to evolve into a less homogeneous configuration that could justify the phase separation experimentally observed.

The ratio of the Na_2O to CaO has been kept constant for all the compositions studied, therefore it is interesting to analyze how the short range environment of the calcium and the sodium ions is modified by the progressive addition of alumina. The MD simulations pointed out that the introduction of the Al_2O_3 leads to an inhomogeneous distribution of the cations in the glass network and, in particular, the number of sodium ions in the first coordination shell of the calcium decreases going from 1Al to 20Al sample (Table VII). This result suggests that the glass structure is going toward the progressive separation into sodium and calcium rich regions.

As regard the local configuration of the erbium sites, Table VII shows that while the number of Na ions decreases as a function of the alumina concentration in the glass composition, the number of Ca ions progressively increases. These results confirm the tendency of the Er^{3+} ion to be coordinated by calcium instead of Na^+ and this is coherent with the separation of a crystalline phase of $Ca_2Er_8(SiO_4)_6O_2$ experimentally observed, in correspondence of high mol% of Er_2O_3, for erbium containing glasses [23].

TABLE VII Percentage of Na and Ca in the first coordination shell of erbium, calcium and aluminium respectively

Sample	Er-Na	Er-Ca	Ca-Na	Al-Na	Al-Ca
1Al	27.79	10.54	26.97	24.12	2.32
5Al	24.69	21.74	22.70	19.60	1.99
10Al	16.55	20.13	18.58	16.40	2.03
15Al	15.77	21.19	15.64	14.77	2.04
20Al	15.20	26.41	15.29	14.62	2.10

Table VII also reports the percentage of sodium and calcium present in the first coordination shell of the aluminium and it is possible to observe that, notwithstanding the increasing concentration of alumina leads to the general decrease of the number of Na^+ ions in the first coordination shell, the aluminium local environment remains mainly constituted by sodium ion. In particular the percentage of the Na^+ ions is at least 6 times greater than the calcium ions.

This result compares well with the previous ones and allows to confirm the tendency of the glass material to separate a crystalline sodium silico-aluminate (nepheline) phase as experimentally observed by XRD analysis.

Information concerning the crystallisation and the microstructure of the glass-ceramic materials was obtained by a scanning electron microscopy.

In Fig. 8 we report the cross-section of samples 10Al, 15Al and 20Al treated at 1000°C and a surface image of 20Al. It is possible to note that the samples present a surface crystallization even if low alumina contents show a very thin crystalline layer (in the samples containing lower alumina content, $<10\%$, the crystalline layer is not visible). The layer for the 15Al sample is about 35 μm while the 20Al sample shows a layer of 150 μm. In this work the nucleation and crystal-growth rates of the glass have not been studied in detail but it is possible to confirm that high amount of alumina increased the crystallisation kinetics of the samples studied. Fig. 8d shows that the microstructure of the 20Al sample surface is quite homogeneous since big crystals of nepheline are grown, which formed a microstructure like “domains”.

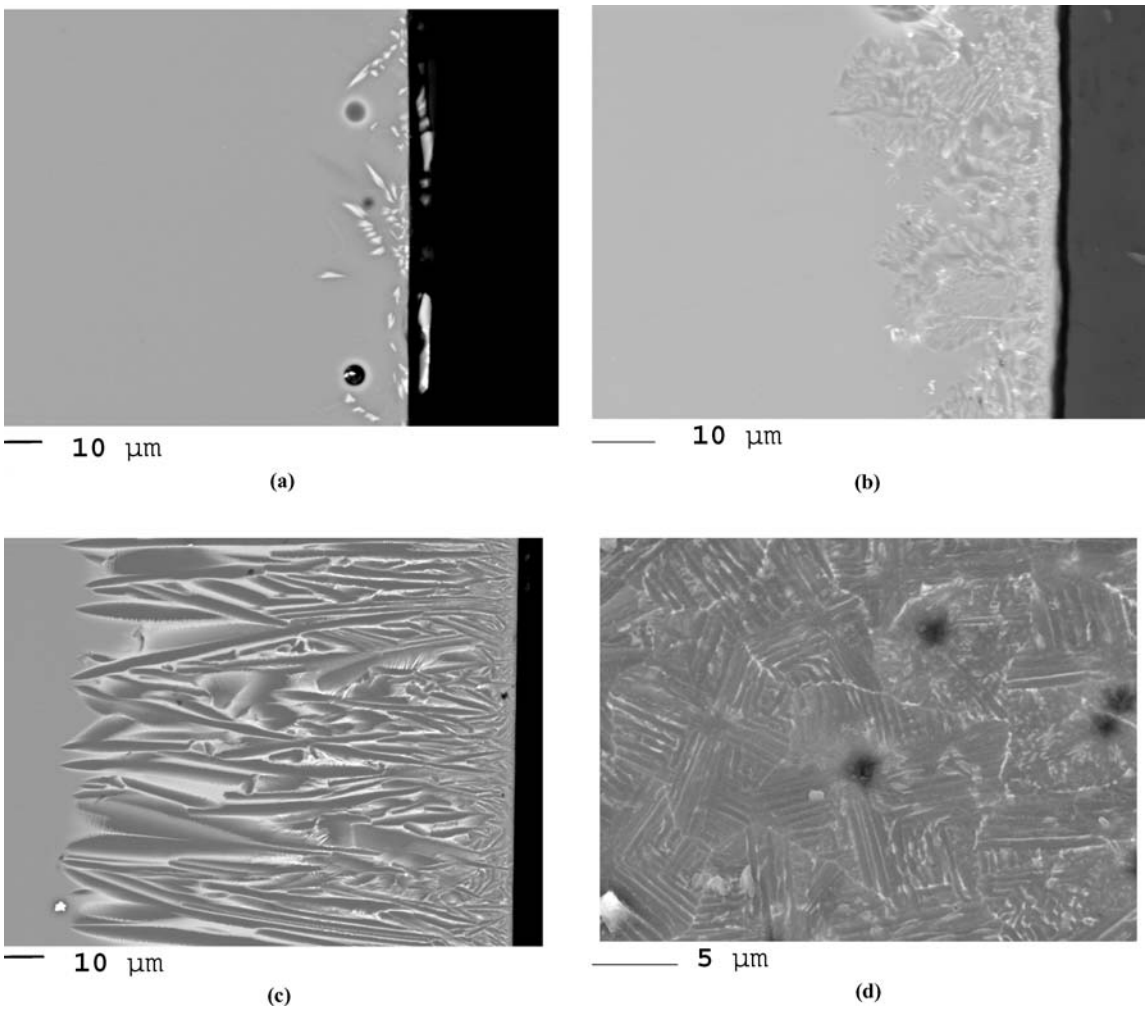

Figure 8 SEM images of samples treated at 1000°C for 30 min: (a) 10Al, (b) 15Al, (c) 20Al cross-section; (d) 20Al surface microstructure.

4. Conclusions

The network former role played by the aluminium in the glass structure has been confirmed by the experimental and MD results. The effect of the alumina addition became significant for a concentration greater than 10 mol% of Al_2O_3, leading to the increase of the glass compactness.

The MD simulations pointed out that the introduction of the Al_2O_3 leads to an inhomogeneous distribution of the cations in the glass network and, in particular, the number of sodium ions in the first coordination shell of the calcium decreases going from the 1Al to 20Al sample. This result suggests that the glass structure is going toward the progressive separation into sodium and calcium rich regions. In fact the thermal stability of the glass decreased since a relevant crystallization of a nepheline phase occurred. Increasing concentration of Al_2O_3 affects also the local configuration of the Er^{3+} leading to distorted octahedra and promoting a random distribution of this cation in the glass network.

References

1. M. NAKAZAW, A. Y. KIMURA and K. SUZUKI, *Appl. Phys. Lett.* **54** (1989) 295.
2. S. TANABE, S. YOSHII, K. HIRAO and N. SOGA, *Phys. Rev.* **B45** (1992) 4620.
3. L. LI, H. LI, M. QIAN and D. M. STRACHAN, *J. Non Cryst. Solids* **281** (2001) 189.
4. G. C. RIGHINI, S. PELLI, M. BRONCI, M. FERRARI, C. DUVERGER, M. MONTAGNA and R. DALL'IGNA, *J. Non-Cryst. Solids* **284** (2001) 223.
5. L. BIGOT, A. M. JURDYC, B. JACQUIER, L. GASCA and D. BAYART, *Phys. Rev.* **B 66** (2002) 214204.
6. E. SNOEKS, G. N. VAN DEN HOVEN, A. POLMAN, B. HENDRIKSEN, M. B. J. DIEMEER and F. PRIOLO, *J. Opt. Soc. Am. B* **12**(8) (1995).
7. G. C. RIGHINI, M. BRENCI, M. A. FORASTIERE, S. PELLI, G. RICCI, G. NUNZI CONTI, N. PEYGHAMBARIAN, M. FERRARI and M. MONTAGNA, *Philos Magazine B* **82** (6) (2002) 721.
8. M. A. MARCUS and A. POLMAN, *J. of Non Cryst. Solids* **136** (1991) 260–265.
9. S. TANABE and T. HANADA, *J. Non Cryst. Solids* **196** (1996) 101.
10. S. BERNESCHI, M. BETTINELLI, M. BRENCI, G. NUNZI CONTI, S. PELLI, S. SEBASTIANI, C. SILIGARDI, A. SPEGHINI, G. C. RIGHINI, *J. of Non-Cryst. Solids* **351** (2005) 1747–1753.
11. M. B. VOLF in "Mathematical Approach to Glass" (Elsevier, Prague, Czech Republic, 1988), pp. 54–66.
12. A. BONAMARTINI CORRADI, V. CANNILLO, M. MONTORSI, C. SILIGARDI and A. N. CORMACK, *J. Non Cryst. Solids* **351** (2005) 1185–1191.

13. B. VESSAL, M. AMINI and C. R. A. CATLOW, *J. Non Cryst. Solids* **159** (1993) 184.
14. J. GALE, *General Utility Lattice Program User Manual-Library of Potentials*, Version 1.3.
15. A. N. CORMACK and Y. CAO, *Mol. Eng.* **6** (1996) 183.
16. B. PARK, H. LI and L. RENÉ CORRALES, *J. Non Cryst. Solids* **297** (2002) 220.
17. K. VOLLMAYR, W. KOB and K. BINDER, *Phys. Rev B.* **54** (1996)15808.
18. A. BONAMARTINI CORRADI, V. CANNILLO and M. MONTORSI, *Mat Eng.* **14** (2003) 87.
19. A. PAUL in "Chemistry of Glasses" (Chapman and Hall, London New York, 1982) pp. 51–63.
20. N. SCHOLZE, *Glas*, (Springer, Berlin-Heidelberg-New York, 1977).
21. M. MONTORSI, M. C. MENZIANI, C. LEONELLI, G. C. PELLACANI and A. N. CORMACK, *Molecular Simulation* **24** (2000) 157.
22. A. K. VARSHNEYA in "Fundamentals of Inorganic Glasses" (Academic Press, San Diego, CA, USA, 1994), pp. 87–96.
23. A. BONAMARTINI CORRADI, V. CANNILLO, M. MONTORSI and C. SILIGARDI, to be submitted.
24. J. V. BH. RAO, *Phys. Chem. Glasses* **4** (1963) 26.
25. A. RUBY, *J. Phys. B* **22** (1972) 1187.

Received 01 March
and accepted 03 August 2005